Crystallization Behavior, Nanostructure and Magnetic Properties of Melt-spun $(Nd,Pr,Dy)_2(Fe,Co,Mo)_{14}B/\alpha$-Fe Nanocomposite Magnets

B. Z. Cui [1, 2] *, K. Han [1], Y. Zhang [3], J. P. Liu [2], H. Garmestani [1, 4], S. Liu [5], H. Schneider-Muntau [1]

[1.] National High Magnetic Field Laboratory, Florida State University, Tallahassee, FL 32310

[2.] Department of Physics, University of Texas at Arlington, Arlington, TX 76019

[3.] Department of Physics and Astronomy, University of Delaware, Newark, DE 19716

4. School of Materials Science and Engineering, Georgia Institute of Technology, Atlanta, GA 30332

5. Magnetics Laboratory, University of Dayton, Dayton, OH 45469

Abstract

The relationship between the crystallization behavior, phase evolution, nanostructure, exchange coupling and hard magnetic properties of melt-spun $Nd_{2.4}Pr_{5.6}Dy_1Fe_{85}B_6$ and $Nd_{2.4}Pr_{5.6}Dy_1Fe_{78}Co_6Mo_1B_6$ nanocomposites has been studied. All the $Nd_{2.4}Pr_{5.6}Dy_1Fe_{85}B_6$ alloys annealed for 30 s at 565°C or above contain nanostructured α-Fe and $Nd_2Fe_{14}B$-type (2:14:1) phases, whereas $Nd_{2.4}Pr_{5.6}Dy_1Fe_{78}Co_6Mo_1B_6$ alloys annealed at 600°C or below are mainly composed of α-Fe and a metastable 1:7 phase with a $TbCu_7$ structure. A small amount of 2:14:1 phase forms after annealing at 600°C. When annealed at 640°C or above, the hard phase in $Nd_{2.4}Pr_{5.6}Dy_1Fe_{78}Co_6Mo_1B_6$ alloys is the 2:14:1 phase rather than the 1:7 phase. The differences in magnetic properties of the $Nd_{2.4}Pr_{5.6}Dy_1Fe_{85}B_6$ and $Nd_{2.4}Pr_{5.6}Dy_1Fe_{78}Co_6Mo_1B_6$ nanocomposites at different anneal temperatures result from the different nanostructures, exchange coupling and phase components present in the alloys, in particular from the different amount of the 1:7 phase.

Index terms: magnetic properties, nanostructure, phase transformation, 1:7 and 2:14:1 phases

* Correspondence Address:
Dr. Baozhi Cui
National High Magnetic Field Laboratory,
Florida State University,
1800 East Paul Dirac Drive,
Tallahassee, FL 32310-4005
Tel: 850-6451241, Fax: 850-6440867
Email: cuibz@yahoo.com

I. INTRODUCTION

Because of their high remanence, extremely high theoretically predicted maximum magnetic energy product and low content of rare earth, nanocomposite magnets have drawn extensive attention for the development of novel permanent magnets with high magnetic performance [1]-[5]. The magnetic properties of the nanocomposite magnets depend strongly on the type of nanostructure, e.g. phases present, crystallite size and shape, distribution of the magnetic grains, defect density and crystallographic texture [1]-[5]. Elemental additions to the nanocomposites have been extensively applied in order to modify these nanostructural factors and hence improve the magnetic properties [3], [4], [6], [7]. On the other hand, recent studies in the melt-spun $Pr_2Fe_{14}B/\alpha$-Fe-nanocomposites have shown that the amorphous precursors usually transit to a 2:14:1 hard phase via metastable phases, such as a 1:7 phase with a $TbCu_7$ structure or a $Pr_2Fe_{23}B_3$ phase, which eventually controls the kinetics of the nucleation and growth of the desired 2:14:1 phase [8]-[9]. The presence of the metastable phases will greatly affect the nanostructure, exchange coupling and magnetic properties of the nanocomposites. In the present work, the crystallization behavior, phase evolution, nanostructure exchange coupling and magnetic properties of melt-spun $Nd_{2.4}Pr_{5.6}Dy_1Fe_{85}B_6$ and $Nd_{2.4}Pr_{5.6}Dy_1Fe_{78}Co_6Mo_1B_6$ nanocomposites are discussed.

II. EXPERIMENT

$Nd_{2.4}Pr_{5.6}Dy_1Fe_{85}B_6$ and $Nd_{2.4}Pr_{5.6}Dy_1Fe_{78}Co_6Mo_1B_6$ ingots were prepared by induction melting under purified argon. The ribbons were prepared by melt spinning in which the molten alloys were quenched on the surface of a molybdenum wheel at a rotation speed of 35 m/s. Before annealing, the melt-spun ribbons were ball milled in acetone for 1 h in a low-energy ball mill to form powders with an average particle size of less than 44 μm. The melt-spun samples were annealed under purified He atmosphere at temperatures ranging from 550 to 720°C for 30 s at a heating rate of 15°C/min in a magnetic field of 1.2 T. Magnetic annealing with a magnetic field of 1.2 T was applied for all of the samples in this study, as it was reported that magnetic annealing resulted in an improvement in the magnetic properties of nanocomposites, compared with an anneal without a magnetic field [10].

The nanostructure and phase components of the samples were studied by x-ray diffraction (XRD) using Cu-Kα radiation and a JEOL JEM-2000FX-type transmission

electron microscopy (TEM). The average grain sizes of α-Fe and 2:14:1 phases were calculated from the Fe (110) and $Nd_2Fe_{14}B$ (410) diffraction peaks using the Scherrer formula. The crystallization behaviors of the as-spun alloys were studied using a Perkin-Elmer DSC7 differential scanning calorimeter (DSC) at a heating rate of 20°C/min. The absolute errors of the measurements for average grain sizes and crystallization temperature T_{cr} were less than ± 2 nm and ± 1°C, respectively. The Curie temperature T_c of the hard phases was obtained from thermomagnetic curves measured by a vibrating sample magnetometer (VSM). For the magnetic measurement at room temperature, the powder specimens were embedded in epoxy resin with an approximate weight ratio of 1:1 between the magnetic powders and the resin. The magnetic properties were measured by the VSM with fields up to 1.5 T. Before demagnetization curves were measured by the VSM, the samples were first magnetized in a pulsed field of 10 T. The results of the magnetic measurements for the powders were corrected using an experimentally determined effective demagnetization factor of 0.28.

III. RESULTS AND DISCUSSION

Fig. 1 shows x-raydiffractograms for the melt-spun $Nd_{2.4}Pr_{5.6}Dy_1Fe_{85}B_6$ alloys before annealing and after annealing at several temperatures. The as-spun $Nd_{2.4}Pr_{5.6}Dy_1Fe_{85}B_6$ sample is composed of a mixture in which a small amount of nanostructured α-Fe and $(Nd,Pr,Dy)_2Fe_{14}B$ nanocrystalline are embedded in an amorphous matrix. The average sizes measured by XRD of the α-Fe and $(Nd,Pr,Dy)_2Fe_{14}B$ crystallites were 8 and 18 nm, respectively. The as-spun samples show very low hard magnetic properties because of the presence of a large amount of magnetically soft amorphous matrix, ${}_iH_c$ = 0.7 kOe; B_r = 9.3 kGs; and $(BH)_{max}$ = 5.8 MGOe. Annealing at 565°C or above for 30 s leads to the formation of a mixture of nanostructured α-Fe and $(Nd,Pr,Dy)_2Fe_{14}B$ phases. After annealing, the average grain size of α-Fe and 2:14:1 phases are in the range of 10 – 17 nm and 20 - 25 nm, respectively.

Fig. 2 shows x-raydiffractograms for the melt-spun $Nd_{2.4}Pr_{5.6}Dy_1Fe_{78}Co_6Mo_1B_6$ samples before annealing and after annealing at selected temperatures. In contrast to the $Nd_{2.4}Pr_{5.6}Dy_1Fe_{85}B_6$ sample, the as-spun $Nd_{2.4}Pr_{5.6}Dy_1Fe_{78}Co_6Mo_1B_6$ sample is composed of a small amount of α-Fe with size of 8 nm and a metastable $(Nd,Pr,Dy)(Fe,Co,Mo)_7$ (1:7) phase embedded in an amorphous matrix. The as-spun $Nd_{2.4}Pr_{5.6}Dy_1Fe_{78}Co_6Mo_1B_6$

sample is magnetically soft and its magnetic properties are very low, ${}_iH_c$ = 0.2 kOe, B_r = 8.7 kGs, and $(BH)_{max}$ = 1.2 MGOe. Annealing at 550°C for 30 s only improves the crystal quality of the α-Fe and 1:7 phases but no tetragonal $(Nd,Pr,Dy)_2(Fe,Co,Mo)_{14}B$ hard phase can be detected. After annealing at 600°C for 30 s, the alloy is still mainly composed of α-Fe and 1:7 phases, accompanied by a small amount of 2:14:1 phase. When the anneal temperature is increased to 640°C, no 1:7 phase can be detected by XRD while the amount of the 2:14:1 phase increases with further increasing the annealing temperature.

From the results of TEM observations, it can be seen that the nanostructures in the $Nd_{2.4}Pr_{5.6}Dy_1Fe_{85}B_6$ and $Nd_{2.4}Pr_{5.6}Dy_1Fe_{78}Co_6Mo_1B_6$ samples annealed at 640°C or above are composed of uniformly distributed α-Fe and 2:14:1 nanograins with grain size from 10 to 35 nm. However, it should be noted that, even after the samples are annealed at 640°C or above, there are still some amorphous phases left in both $Nd_{2.4}Pr_{5.6}Dy_1Fe_{85}B_6$ and $Nd_{2.4}Pr_{5.6}Dy_1Fe_{78}Co_6Mo_1B_6$ samples, which can be detected by TEM (not shown here). A representative TEM bright field image and corresponding selected area diffraction of $Nd_{2.4}Pr_{5.6}Dy_1Fe_{85}B_6$ alloy annealed at 680°C for 30 s is shown in Fig. 3.

From the results of the thermomagnetic curves, it is seen that the T_c of the hard phases remains the same (320°C) in the $Nd_{2.4}Pr_{5.6}Dy_1Fe_{85}B_6$ alloy annealed for 30 s at 565°C or above, which corresponds to the $(Nd,Pr,Dy)_2Fe_{14}B$ phase. In contrast, for the $Nd_{2.4}Pr_{5.6}Dy_1Fe_{78}Co_6Mo_1B_6$ alloy, with increasing the annealing temperature from 550°C to 600°C and 640°C, the T_c of the hard phases increases monotonously from 415°C to 430°C and 445°C, and then keeps constant at 445°C, which is T_c of $(Nd,Pr,Dy)_2(Fe,Co,Mo)_{14}B$ phase, even with further increasing the annealing temperatures. The change of T_c of the hard phases in the $Nd_{2.4}Pr_{5.6}Dy_1Fe_{78}Co_6Mo_1B_6$ samples annealed at different temperatures is due to the different magnetic phases present in the alloys as mentioned above. It should be noted, that only one T_c of the 1:7 phase, rather than two separate T_c of the 1:7 and 2:14:1 phases, was observed at $Nd_{2.4}Pr_{5.6}Dy_1Fe_{78}Co_6Mo_1B_6$ alloy annealed at 600°C, though there are two hard phases (1:7 and 2:14:1) in this alloy. This is mainly due to the too small amount of the 2:14:1 phase and the low resolution of the thermomagnetic measurement by VSM. The monotonic increase of the Curie temperature of the hard phase with increasing the annealing temperature from 550 to 640°C is mainly attributed to the change of the concentration of the matrix 1:7 phases, resulting from the continuous phase transformation from the 1:7 to the 2:14:1 structure [11]-[12].

In comparison with the $Nd_{2.4}Pr_{5.6}Dy_1Fe_{85}B_6$ alloy, the observable increase of T_c of the 2:14:1 phase in the $Nd_{2.4}Pr_{5.6}Dy_1Fe_{78}Co_6Mo_1B_6$ alloy originates from the reinforced Fe-Fe ferromagnetic exchange interaction in the 2:14:1 phase, implying both Co and Mo can enter into the sublattice occupied primarily by Fe in the hard tetragonal phase [4], [13].

DSC curves of the as-spun $Nd_{2.4}Pr_{5.6}Dy_1Fe_{85}B_6$ and $Nd_{2.4}Pr_{5.6}Dy_1Fe_{78}Co_6Mo_1B_6$ alloys are shown in Fig. 4. It can be seen that, there are two exothermic peaks in the DSC curve of $Nd_{2.4}Pr_{5.6}Dy_1Fe_{85}B_6$ alloy while there are three exothermic peaks in that of $Nd_{2.4}Pr_{5.6}Dy_1Fe_{78}Co_6Mo_1B_6$ alloy. The first peak at low temperature can be attributed to the precipitation of α-Fe from the matrix for both materials. T_{cr} of α-Fe for $Nd_{2.4}Pr_{5.6}Dy_1Fe_{85}B_6$ is slightly higher than the other probably because of the higher Fe content in this alloy. For the $Nd_{2.4}Pr_{5.6}Dy_1Fe_{85}B_6$ alloy, the second exothermic peak corresponds to the crystallization of the amorphous matrix into the $(Nd,Pr,Dy)_2Fe_{14}B$ phase. The crystallization temperatures T_{cr} of α-Fe and $(Nd,Pr,Dy)_2Fe_{14}B$ phases are 522°C and 590°C, respectively. For $Nd_{2.4}Pr_{5.6}Dy_1Fe_{78}Co_6Mo_1B_6$ alloy, the second exothermic peak corresponds to the formation of a metastable 1:7 phase from the amorphous matrix. The third peak corresponds to a phase transformation from a $TbCu_7$ structure to a $Nd_2Fe_{14}B$ structure. T_{cr} of the α-Fe, 1:7 and 2:14:1 phases are 529°C, 603°C and 635°C, respectively.

Fig. 5 gives the dependence of the intrinsic coercivity $_iH_c$, the maximum magnetic energy product $(BH)_{max}$ and the remanence B_r on the annealing temperature for both, $Nd_{2.4}Pr_{5.6}Dy_1Fe_{85}B_6$ and $Nd_{2.4}Pr_{5.6}Dy_1Fe_{78}Co_6Mo_1B_6$ alloys, annealed for 30 s. It can be seen that, with increasing the annealing temperatures, $_iH_c$ and $(BH)_{max}$ increase then decrease for both materials. It is known that the metastable 1:7 phase has a non-uniaxial magnetocrystalline anisotropy [14], [15], so the presence of 1:7 phase just degrades the hard magnetic properties of the nanocomposite magnets. Low $_iH_c$ and $(BH)_{max}$ and high B_r of $Nd_{2.4}Pr_{5.6}Dy_1Fe_{78}Co_6Mo_1B_6$ alloys annealed at 600°C or below are due to the existence of a large amount of α-Fe and 1:7 phases and even some left amorphous matrix. However, the increase of $_iH_c$ after annealing at 600°C indicates the presence of a small amount of the 2:14:1 hard phase responsible for the magnetic hardening. Especially, a sharp increase of $_iH_c$ and $(BH)_{max}$ after annealing at 640°C corresponds to the complete formation of the 2:14:1 phase. At relatively high annealing temperatures (660 - 720°C), although a complete solid-state phase transformation from the 1:7 to the 2:14:1 structure can occur, the α-Fe grains become too coarse, which diminishes the exchange coupling between the

soft and hard nanograins and hence degrades the hard magnetic properties [2], [4], [5], [16]. After the samples are annealed at 660°C, the formation of 2:14:1 phase in the $Nd_{2.4}Pr_{5.6}Dy_1Fe_{78}Co_6Mo_1B_6$ alloy is complete (cf. Fig.s 1 and 4) and the average grain size of α-Fe is relatively small. Thus, ${}_iH_c$ and $(BH)_{max}$ attain their maxima at 660°C.

On the other hand, although T_{cr} for formation of 2:14:1 in $Nd_{2.4}Pr_{5.6}Dy_1Fe_{85}B_6$ is about 45°C lower than in $Nd_{2.4}Pr_{5.6}Dy_1Fe_{78}Co_6Mo_1B_6$, the transformation from amorphous phase to hard 2:14:1 magnetic phase is incomplete at relatively low annealing temperatures (565 - 640°C). Therefore, there still is some amorphous phase left in the alloys and the volume fraction of $(Nd,Pr,Dy)_2Fe_{14}B$ is relatively small. Thus, ${}_iH_c$ and $(BH)_{max}$ is relatively low. At relatively high annealing temperatures (640 - 720°C), the decrease in ${}_iH_c$ and $(BH)_{max}$ is due to the coarsening of α-Fe grains [2], [4], [5], [16]. Thus, ${}_iH_c$ and $(BH)_{max}$ attain their maxima at 640°C.

Fig. 6 shows the demagnetization curves of the melt-spun $Nd_{2.4}Pr_{5.6}Dy_1Fe_{85}B_6$ and $Nd_{2.4}Pr_{5.6}Dy_1Fe_{78}Co_6Mo_1B_6$ alloys annealed at 660°C for 30 s. The two materials demonstrate typical but different magnetization behavior of nanocomposite magnets without any contracted shape, indicating that the exchange coupling between the soft and hard grains has been realized. The demagnetization curve of the $Nd_{2.4}Pr_{5.6}Dy_1Fe_{78}Co_6Mo_1B_6$ alloy shows more rectangularity than that of $Nd_{2.4}Pr_{5.6}Dy_1Fe_{85}B_6$ alloy. B_r and $(BH)_{max}$ of $Nd_{2.4}Pr_{5.6}Dy_1Fe_{78}Co_6Mo_1B_6$ alloys after annealing at 660°C or above are higher while their ${}_iH_c$ are lower than those of $Nd_{2.4}Pr_{5.6}Dy_1Fe_{85}B_6$ alloys annealed at the same temperatures.

In comparing our structural and magnetic results, it appears that the presence of the 1:7 phase and exchange coupling determines the magnetic properties for $Nd_{2.4}Pr_{5.6}Dy_1Fe_{85}B_6$ and $Nd_{2.4}Pr_{5.6}Dy_1Fe_{78}Co_6Mo_1B_6$ alloys annealed at 660°C or above. It has been reported that the addition of Co and Mo to $Nd_{8.4}Fe_{87.1}B_{4.5}$ alloys prepared by mechanical alloying enhanced exchange coupling through improvements of the nanostructure, such as refinement of grain, promotion of a more uniform distribution of the soft and hard magnetic grains, and reduction of the defects on the grain boundaries, etc [4]. This may be the main reason why $Nd_{2.4}Pr_{5.6}Dy_1Fe_{78}Co_6Mo_1B_6$ alloys annealed at 660°C or above have a better rectangularity of the demagnetization curves and higher remanence, and, in turn, higher $(BH)_{max}$. On the other hand, although it cannot be detected by XRD patterns due to the overlapping of the diffraction peaks for the 1:7 and 2:14:1 phases and the minor amount of 1:7 phase, the 1:7 phase still possibly exists in the $Nd_{2.4}Pr_{5.6}Dy_1Fe_{78}Co_6Mo_1B_6$

alloys annealed at 660°C or above, which can be detected by sensitive Mössbauer spectroscopy measurements [4], [17]. This may be the main reason why ${}_iH_c$ of the $Nd_{2.4}Pr_{5.6}Dy_1Fe_{78}Co_6Mo_1B_6$ alloy annealed at 660°C or above is lower than that of the $Nd_{2.4}Pr_{5.6}Dy_1Fe_{85}B_6$ alloy. The magnetic properties of nanocomposites are determined by the competence of enhanced exchange coupling and the presence of 1:7 phase.

This work was supported by DARPA through ARO under grant DAAD19-03-1-0038. Dr. B. Z. Cui thanks the financial supports from Prof. H. Garmestani at GATECH.

REFERENCES

[1] A. Manaf, R. A. Buckley, H. A. Davies, J. Magn. Magn. Mater. **128**, 302 (1993).

[2] B. Z. Cui, X. K. Sun, L Y. Xiong, W. Liu, Z. D. Zhang, Z. Q. Yang, A. M. Wang and J. N. Deng, J. Mater. Res. **16**, 709 (2001).

[3] P. Crespo, V. Neu, and L. Schultz, J. Phys. D: Appl. Phys. **30**, 2298 (1997).

[4] B. Z. Cui, X. K. Sun, L. Y. Xiong, S. T. Tang, X. X. Zhang, W Liu, D. Y. Geng, and Z. D. Zhang, J. Alloys Compd. **340**, 242 (2002).

[5] R. Skomski and J. M. D. Coey, Phys. Rev. B **48**, 15812 (1993).

[6] B. Z. Cui, X. K. Sun, W. Liu, Z. D. Zhang, D. Y. Geng, X. G. Zhao, J. P. Liu and D. J. Sellmyer, J. Appl. Phys. **87**, 5335 (2000).

[7] B. Z. Cui, X. K. Sun, W. Liu, Z. D. Zhang, D. Y. Geng and X. G. Zhao, J. phys. D: Applied Physics **33**, 338 (2000).

[8] Z. Q. Jin, H. Okumura, Y. Zhang, H. L. Wang, J. S. Muñoz, and G. C. Hadjipanayis, J. Magn. Magn. Mater. **248**, 216 (2002).

[9] Z. C. Wang, S. Z. Zhou, Y. Qiao, M. C. Zhang, and R. Wang, J. Magn. Magn. Mater. **218**, 72 (2000).

[10] B. Z. Cui, M. Q. Huang, R. H. Yu, A. Kramp, J. Dent, D. D. Miles, and S. Liu, J. Appl. Phys. **93,** 8128 (2003).

[11] B. Z. Cui, X. K. Sun, D. Y. Geng, W. Liu, X. G. Zhao, Z. D. Zhang, Y. C. Sui, and J. W. Liu, J. Alloys and Compds. **293 – 295**, 868 (1999).

[12] B. Z. Cui, X. K. Sun, Y. C. Sui, D. Y. Geng, and Z. D. Zhang, J. Magn. Magn. Mater. **250**, 212 (2002).

[13] W. Rodewald, W. Fernengel, IEEE. Trans. Magn. **24**, 1638 (1988).

[14] A. Navarathna, H. Hegde, R. Rani, and F. J. Cadieu, J. Appl. Phys. **73**, (1993) 6242.

[15] Z. D. Zhang, W. Liu, J. P. Liu and D. J. Sellmyer, J. Phys. D Appl. Phys. **33,** (2000) R217.

[16] E. F. Kneller and R. Hawig, IEEE. Trans. Magn. **27**, (1991) 3588.

[17] B. Z. Cui, Y. C. Sui, X. K. Sun, L Y. Xiong, M. J. O'Shea, and Z. D. Zhang, J. Appl. Phys. **91**, 7881 (2002).

Figure Captions

Fig.1 XRD patterns of the melt-spun $Nd_{2.4}Pr_{5.6}Dy_1Fe_{85}B_6$ samples before annealing, and after annealing at several temperatures in a magnetic field of 1.2 T. The t and n stand for α-Fe and 2:14:1 phases, respectively.

Fig.2 XRD patterns of the melt-spun $Nd_{2.4}Pr_{5.6}Dy_1Fe_{78}Co_6Mo_1B_6$ samples before annealing, and after annealing at several temperatures in a magnetic field of 1.2 T. The t, o and n stand for α-Fe, 1:7 and 2:14:1 phases, respectively.

Fig.3 TEM bright field image and corresponding selected area diffraction of $Nd_{2.4}Pr_{5.6}Dy_1Fe_{85}B_6$ alloy annealed at 680°C for 30 s in a magnetic field of 1.2 T.

Fig.4 DSC curves of the as-spun $Nd_{2.4}Pr_{5.6}Dy_1Fe_{85}B_6$ and $Nd_{2.4}Pr_{5.6}Dy_1Fe_{78}Co_6Mo_1B_6$ alloys.

Fig.5 Dependence of ${}_iH_c$, $(BH)_{max}$ and B_r on annealing temperature for the $Nd_{2.4}Pr_{5.6}Dy_1Fe_{85}B_6$ and $Nd_{2.4}Pr_{5.6}Dy_1Fe_{78}Co_6Mo_1B_6$ alloys annealed for 30 s in a magnetic field of 1.2 T.

Fig.6 Demagnetization curves of the $Nd_{2.4}Pr_{5.6}Dy_1Fe_{85}B_6$ and $Nd_{2.4}Pr_{5.6}Dy_1Fe_{78}Co_6Mo_1B_6$ alloys annealed at 660°C for 30 s in a magnetic field of 1.2 T.

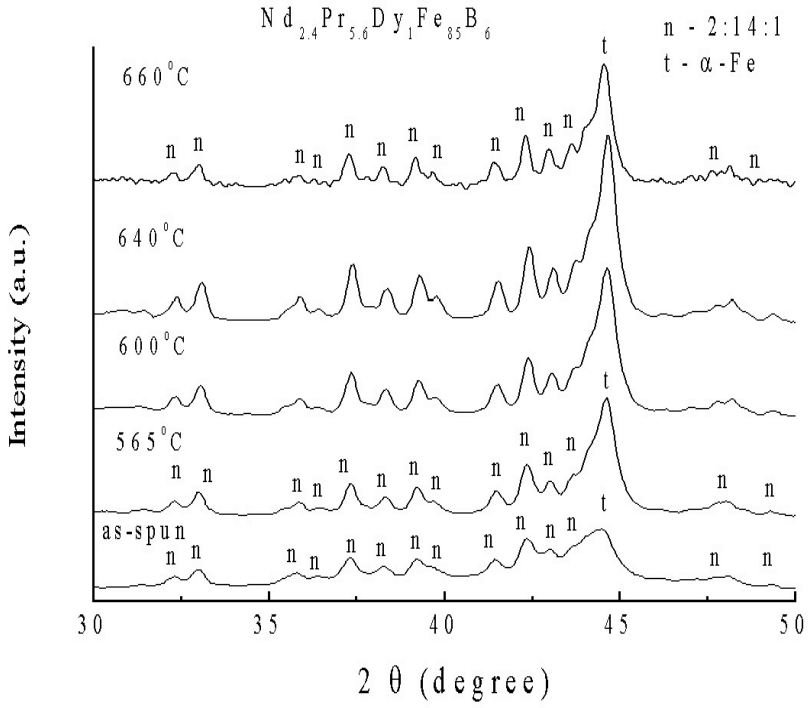
Nd2.4Pr5.6Dy1Fe85B6
n - 2:14:1
t - α-Fe
660°C
640°C
600°C
565°C
as-spun
Intensity (a.u.)
2 θ (degree)
30
35
40
45
50

Fig.1

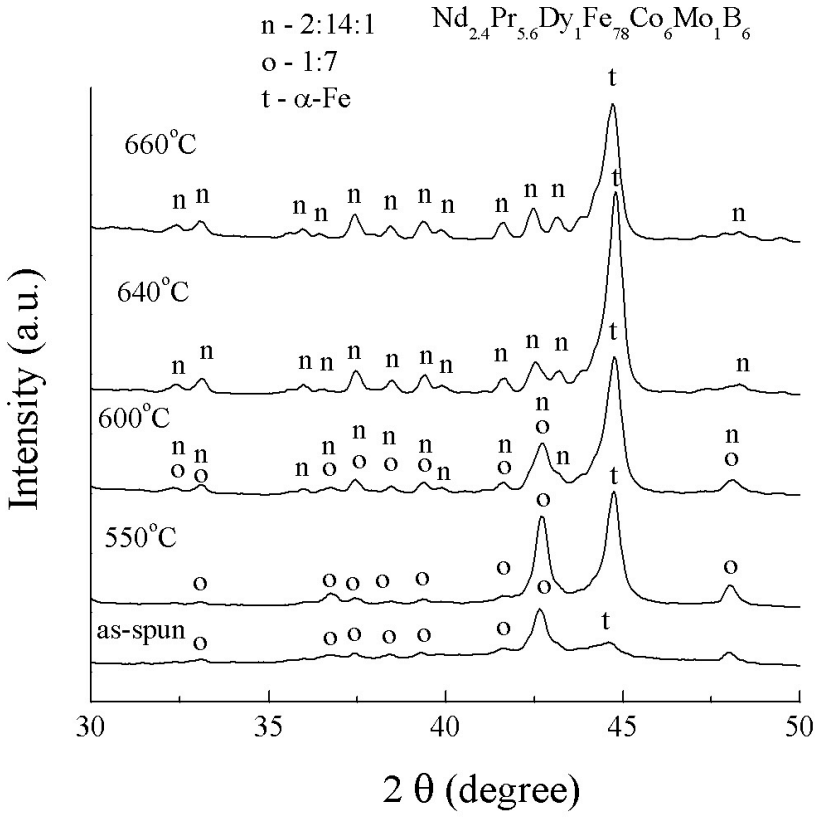
n - 2:14:1
o - 1:7
t - α-Fe
Nd2.4Pr5.6Dy1Fe78Co6Mo1B6
660°C
640°C
600°C
550°C
as-spun
Intensity (a.u.)
2 θ (degree)
30
35
40
45
50

Fig.2

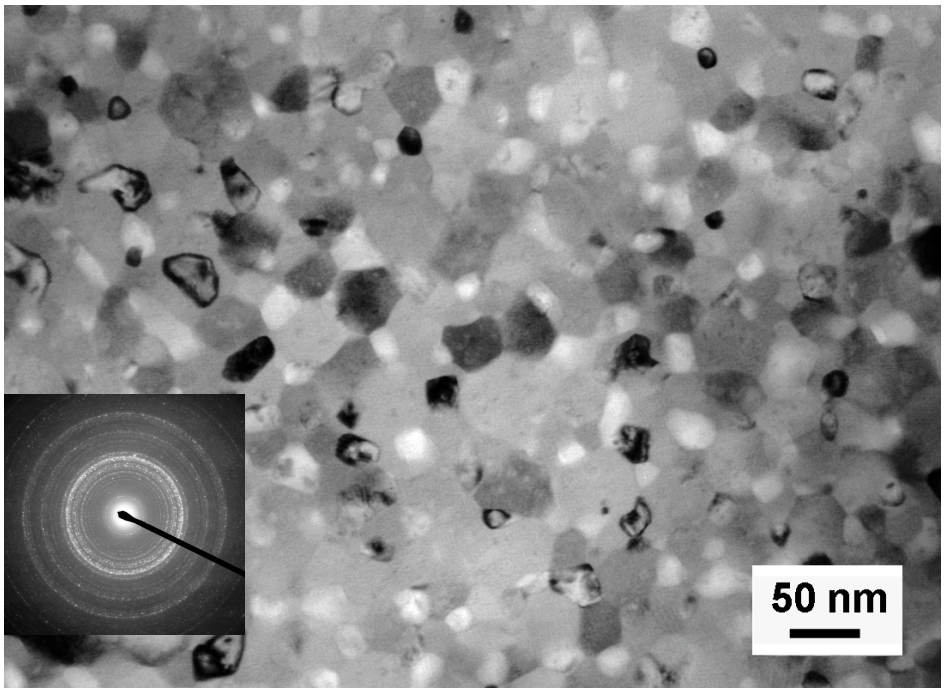

Fig.3

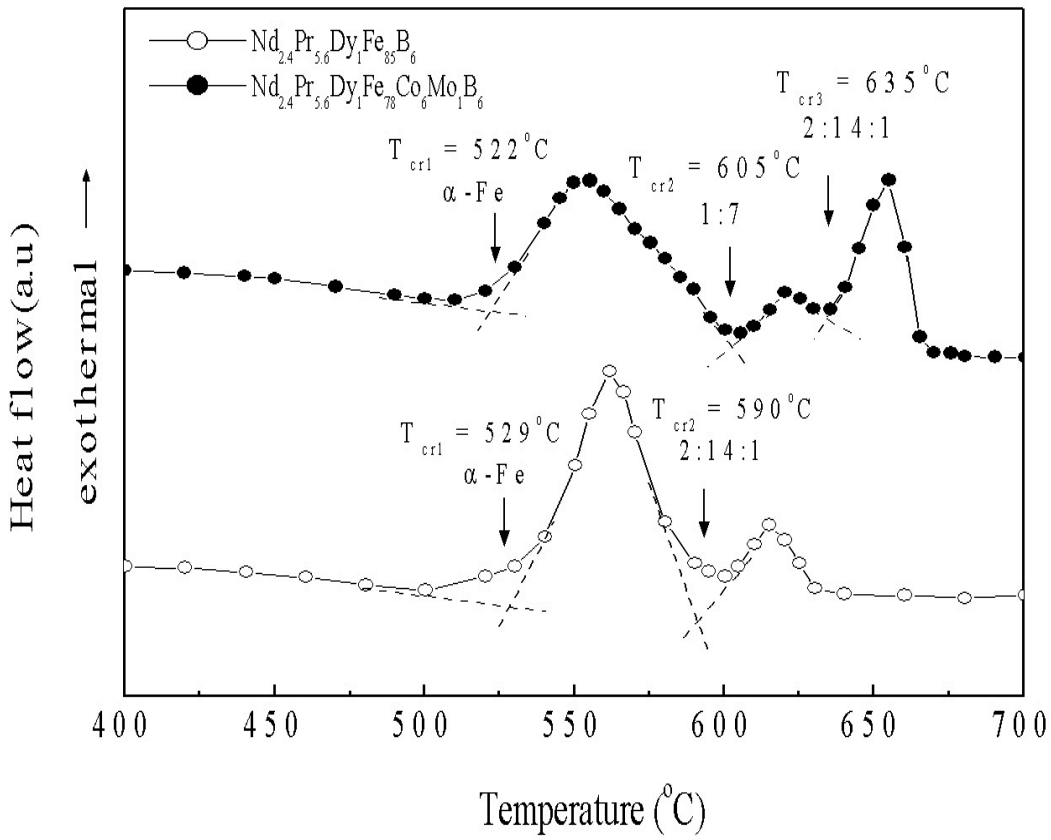
Nd2.4Pr5.6Dy1Fe85B6
Nd2.4Pr5.6Dy1Fe78Co6Mo1B6
Tcr1 = 522°C
α-Fe
Tcr2 = 605°C
1:7
Tcr3 = 635°C
2:14:1
Tcr1 = 529°C
α-Fe
Tcr2 = 590°C
2:14:1
Heat flow(a.u)
exothermal
400
450
500
550
600
650
700
Temperature (°C)

Fig.4

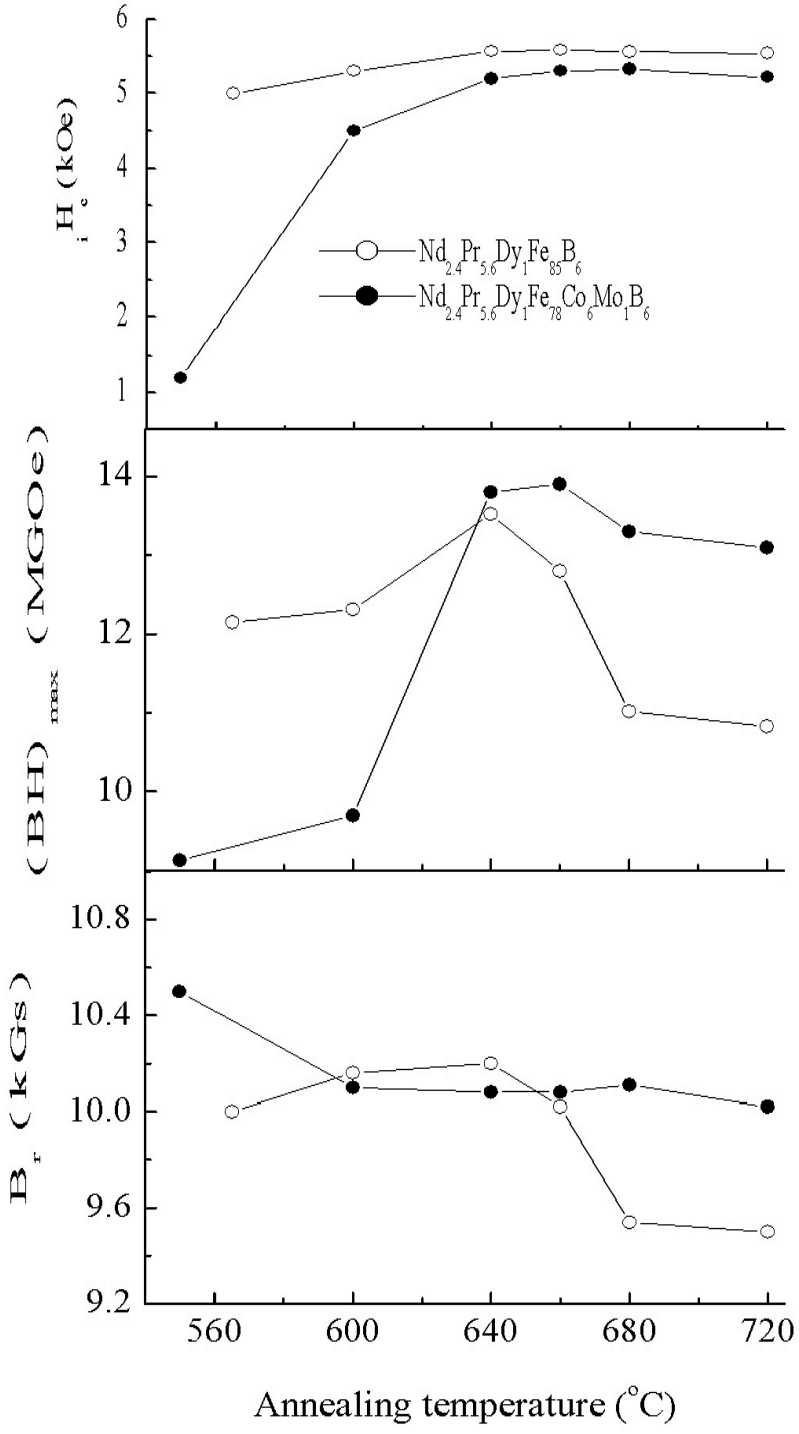
H_{ic} (kOe)
$Nd_{2.4}Pr_{5.6}Dy_1Fe_{85}B_6$
$Nd_{2.4}Pr_{5.6}Dy_1Fe_{78}Co_6Mo_1B_6$
$(BH)_{max}$ (MGOe)
B_r (kGs)
Annealing temperature (°C)

Fig.5

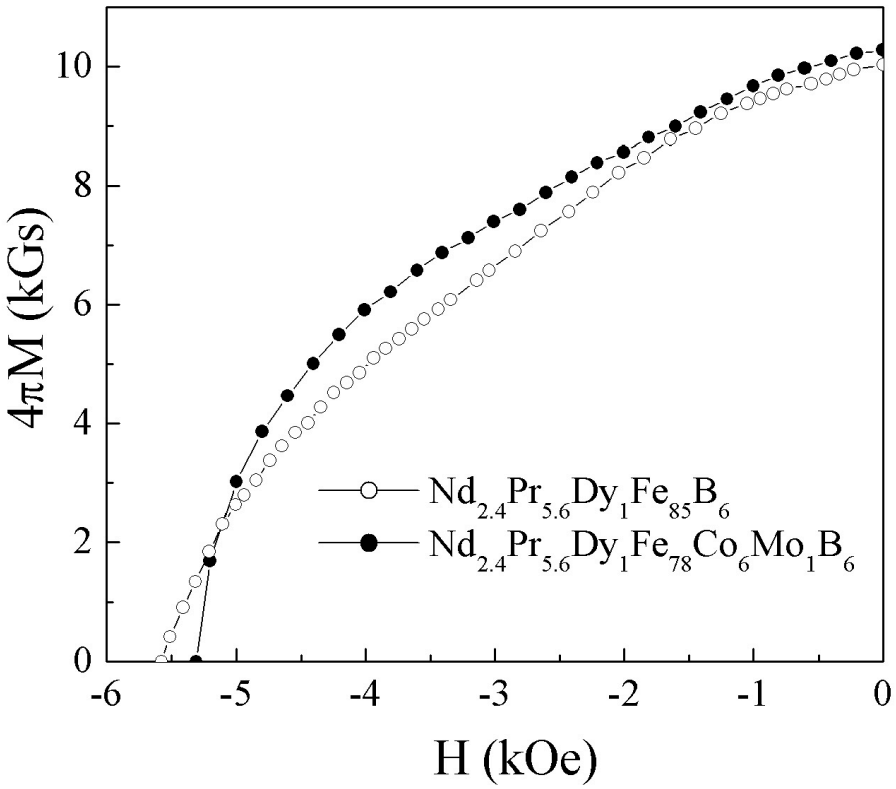
10
8
6
4
2
0
-6
-5
-4
-3
-2
-1
0
4πM (kGs)
H (kOe)
Nd2.4Pr5.6Dy1Fe85B6
Nd2.4Pr5.6Dy1Fe78Co6Mo1B6

Fig.6